NRC Publications Archive
Archives des publications du CNRC

Mid-infrared reflectance spectroscopy of oil sands minerals based on tunable quantum cascade lasers

Harhira, Aissa; Vanier, Francis; Padioleau, Christian; El haddad, Josette; Blouin, Alain

NRC Publications Archive Record / Notice des Archives des publications du CNRC :
https://nrc-publications.canada.ca/eng/view/object/?id=30c94216-723d-4b3e-b21b-96030f091fc9
https://publications-cnrc.canada.ca/fra/voir/objet/?id=30c94216-723d-4b3e-b21b-96030f091fc9

Questions? Contact the NRC Publications Archive team at
PublicationsArchive-ArchivesPublications@nrc-cnrc.gc.ca. If you wish to email the authors directly, please see the first page of the publication for their contact information.

Vous avez des questions? Nous pouvons vous aider. Pour communiquer directement avec un auteur, consultez la première page de la revue dans laquelle son article a été publié afin de trouver ses coordonnées. Si vous n'arrivez pas à les repérer, communiquez avec nous à PublicationsArchive-ArchivesPublications@nrc-cnrc.gc.ca.

National Research Council Canada   Conseil national de recherches Canada

Canada

Paper type: Rapid Communication

Mid-Infrared Reflectance Spectroscopy of Oil Sands minerals based on Tunable Quantum Cascade Lasers

Aïssa Harhira*, Francis Vanier, Christian Padioleau, Josette El Haddad, Alain Blouin

National Research Council Canada, 75 de Mortagne Blvd., Boucherville, Québec, Canada, J4B 6Y4

Corresponding author email: Aissa.Harhira@cnrc-nrc.gc.ca

Abstract

Minerals play an important role in the oil sands extraction efficiency. It is thus important to assess the major mineral abundance in oil sands ores. This paper presents the application of tunable quantum cascade lasers for mid-infrared reflectance spectroscopy on oil sands minerals. The investigations and results show a new tool to determine oil sands mineral type and to determine potentially quartz and clay contents.

Keywords

Mid-infrared spectroscopy, mid-IR, quantum cascade lasers, QCL, oil sands, reflectance spectroscopy

Introduction

Oil sands are the most important heavy oil reserves in Canada. Oil sands consist of bitumen, water, and solid minerals which are mainly quartz and clays. The production of oil from an open-pit oil sands mine requires several steps from mining to refining. Prior to bitumen extraction, it is critical to know the clay content of the oil sands feedstock because these clays can affect the bitumen recovery. Indeed, a high clay content in the feedstock can disrupt the extraction process, decrease the recovery rate, and produce a low-quality froth. Moreover, a high clay content can generate a deleterious waste product called tailings with a negative ecological impact.

Several laboratory techniques have been used for the characterization of minerals in oil sands. X-ray diffraction (XRD) has been used to determine qualitatively the mineralogy of the

bitumen-free oil sands. Quantitative X-ray diffraction (QXRD) has also been used to determine crystalline minerals. Reflectance optical spectroscopy and hyperspectral measurements have been performed to investigate the mineral abundance in oil sands.[1] Combined QXRD and X-ray fluorescence have been used to determine both crystalline and non-crystalline phase in oil sands minerals. Other techniques such as energy-dispersive X-ray spectroscopy (EDX)[2] and laser-induced breakdown spectroscopy (LIBS) have been used to study the elemental composition.[3] K40 gamma spectroscopy is widely used for on-line measurement of clay content but efforts are still needed to provide a reliable quantitative measurement.[4]

Recently, the commercialization of tunable external cavity quantum cascade lasers (ECQCL) emitting in the mid-infrared (mid-IR) range is enabling laser-based mid-IR spectroscopy in many applications[5–6] and offers, in some aspects, serious competition to traditional Fourier transform infrared (FT-IR) spectroscopy.[7] Compared to a broadband light source and an FT-IR spectrometer, tunable ECQCL modules provide a larger spectral power density, hence a better signal-to-noise ratio for the same acquisition time. Moreover, a laser beam can be focused on a smaller spot even at standoff distances, enabling higher spatial resolution mapping of a sample. Published work on ECQCL-based spectroscopy are reported for absorption spectroscopy in gases,[8] in thin liquid layers,[9–10] in pharmaceutical products,[11] for chemical agent detection,[12] and more recently for mineral characterization.[13]

In this paper, we demonstrate ECQCL-based reflectance spectroscopy applied to predict the abundance of quartz and clays in free-bitumen oil sands. We measured each sample at a standoff distance and at several locations to mitigate the sample heterogeneity. Then we investigate if ECQCL-based reflectance spectroscopy can be used to distinguish between high and low quartz to clay ratio oil sands minerals by using the mid-IR spectral signatures. The objective of this work was to assess the potential of using an on-line ECQCL-based sensor system to monitor the quality of the feedstock oil sands.

Experimental Setup

The mid-IR reflectance spectroscopy setup is shown in Figure 1. Figures 1a and b show the top and side view of the setup schematic, respectively. The mid-IR beam is emitted from a Block Engineering LaserTune ECQCL module. The beam is focused on the sample at normal incidence angle using a 1-inch (2.54 cm) gold parabolic mirror. The spot diameter at the sample is 300 μm

and the working distance is 10 cm. The reflected light is collected at an angle of 20° using another 1-inch (2.54 cm) diameter gold parabolic mirror as seen in Figure 1c. The mid-IR light is then focused on a 1x1 mm^2 Infrared Associate FT-IR-16 MCT detector operated at 77 K using liquid nitrogen. The ECQCL module is composed of four tunable lasers in total. Their spectral ranges are separated at 970 cm^{-1}, 1344.7 cm^{-1}, and 1632.4 cm^{-1}. To acquire a reflection spectrum, the center wavelength of the emitted light is continuously tuned across a wavelength range of 5.2 μm to 13.4 μm (745 cm^{-1} to 1920 cm^{-1}) over 0.5 s. The ECQCL module is emitting light pulses of 100 ns duration at a repetition rate of 10 kHz. The peak voltage generated by each reflected light pulse is recorded to form a spectrum of 5000 data points. The raw reflection spectra are smoothed using an 11-points moving average, which was normalized using the diffuse reflection spectrum of slightly pressed KBr powder.
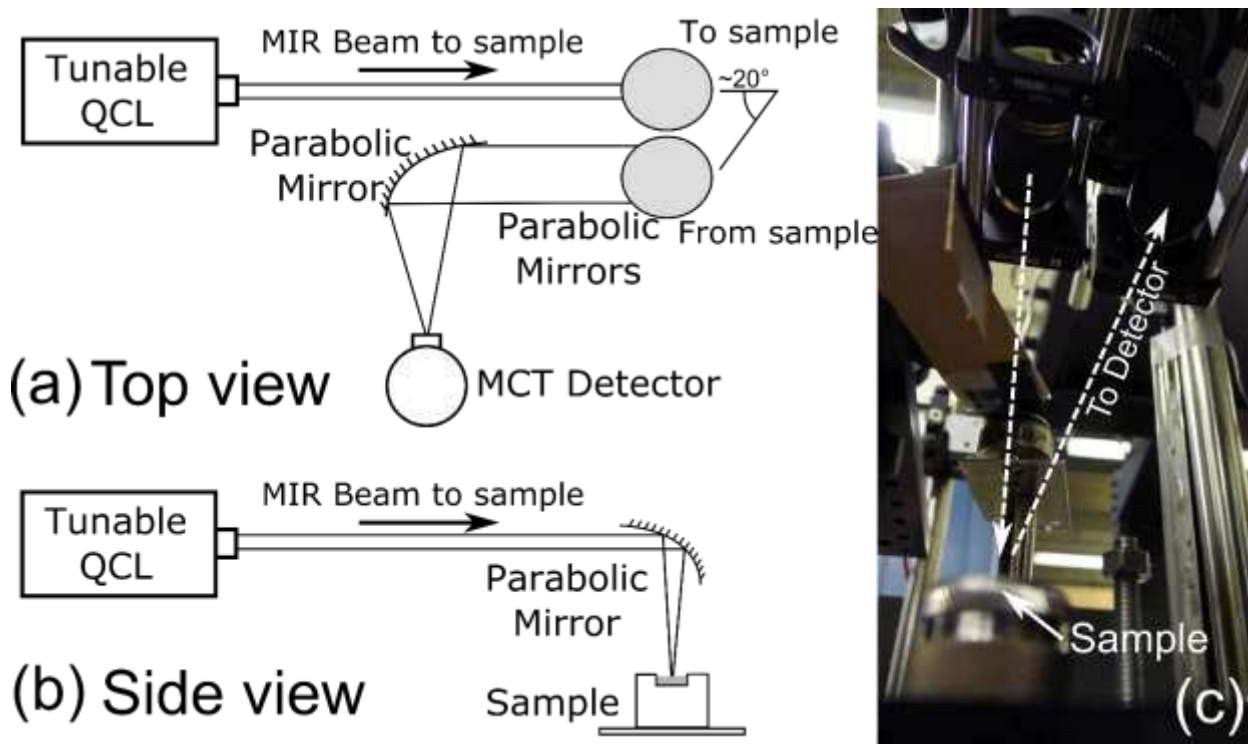

Figure 1. (a) Top view schematic of the mid-IR reflectance setup. (b) Side view of the setup. (c) Photograph from the sample point-of-view.

Eleven oil sands samples classified as high quartz to clay ratio (Q/C) and low quartz to clay ratio samples are used in this work. The oil sands samples were extracted using the standard Soxhlet–Dean and Stark extraction methods with toluene as the solvent. After drying, the

quantitative mineralogy of the bitumen-free oil sands samples was obtained by QXRD analysis. The material is then homogenized for the mid-IR measurements. The total clay content shown in Table I refers to the summation of kaolinite, illite and chlorite contents, and of the content of a mixture of illite–smectite and kaolinite–smectite mixed layers.

Table I. Mineral abundance and quartz to clay ratio (Q/C).

Sample	Quartz (%)	Total Clay (%)	Other Minerals (%)	Quartz to Clay (Q/C) Ratio	Category
1	65.7	24.9	9.4	2.6	Low Q/C
2	69.6	22.5	7.9	3.1	Low Q/C
3	66.6	18.0	15.4	3.7	Low Q/C
4	78.2	14.9	6.9	5.3	Low Q/C
5	81.9	12.3	5.8	6.7	Low Q/C
6	81.7	11.5	6.8	7.1	Low Q/C
7	93.2	3.5	3.3	26.8	High Q/C
8	94.0	2.5	3.5	37.0	High Q/C
9	86.8	2.3	10.9	38.0	High Q/C
10	92.7	2.4	4.9	39.4	High Q/C
11	88.1	2.0	9.9	44.3	High Q/C

Figure 2 shows one of the bitumen-free oil sands sample under the mid-IR reflectance setup. The green and red circles indicate the center and the border of the probed region by the mid-IR beam, respectively. For each oil sands sample, approximately 100 mg of homogenized material is put in a circular holder and is slightly pressed down to obtain a uniform surface as seen in Figure 2. This procedure was repeated five times to obtain five subsamples. Reflection spectra are measured at 36 locations separated by 0.5 mm. The average of 36 reflection spectra is then used to obtain a representative sampling. Figure 3 shows normalized reflection spectra for low Q/C and high Q/C samples. The mid-IR spectra data set consisted of 55 averaged reflection spectra, one for each subsample, belonging to the 11 samples. These measurements were used to evaluate variability of such heterogeneous samples.
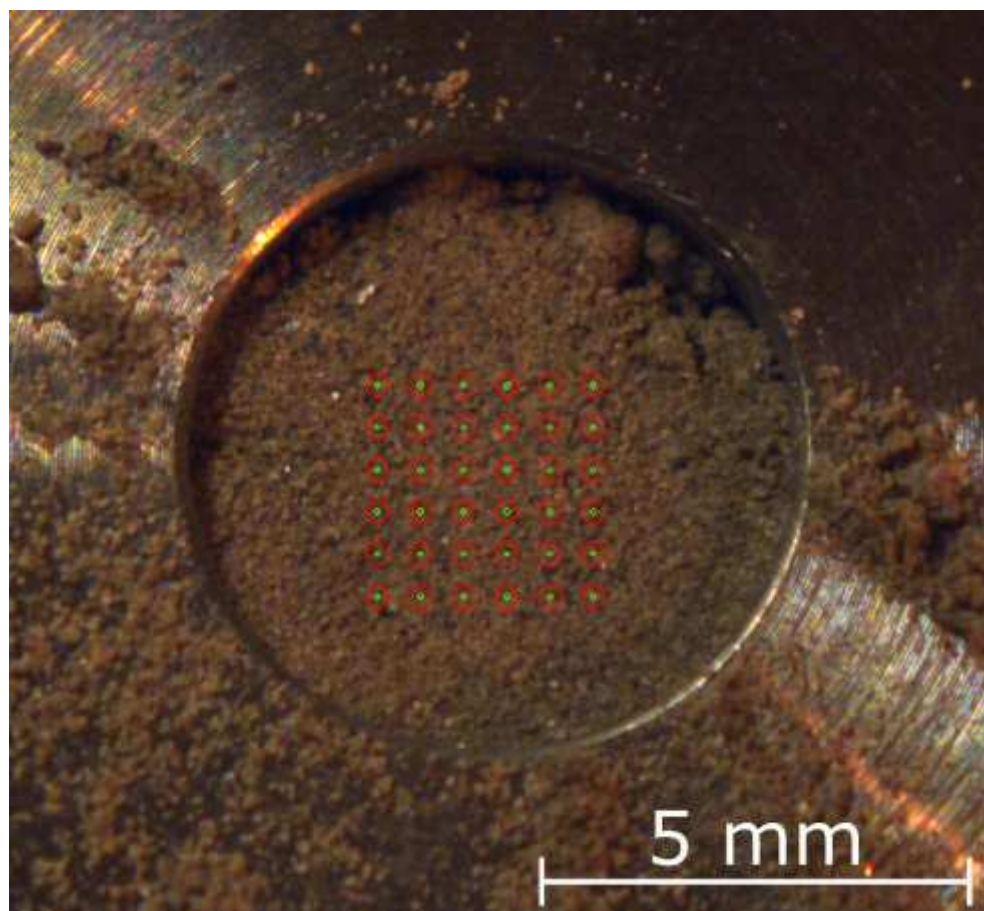
Figure 2. Image of a typical bitumen-free oil sands sample under the mid-IR reflectance setup. The green and red circles indicate the center and the border of the probed region by the mid-IR beam respectively.
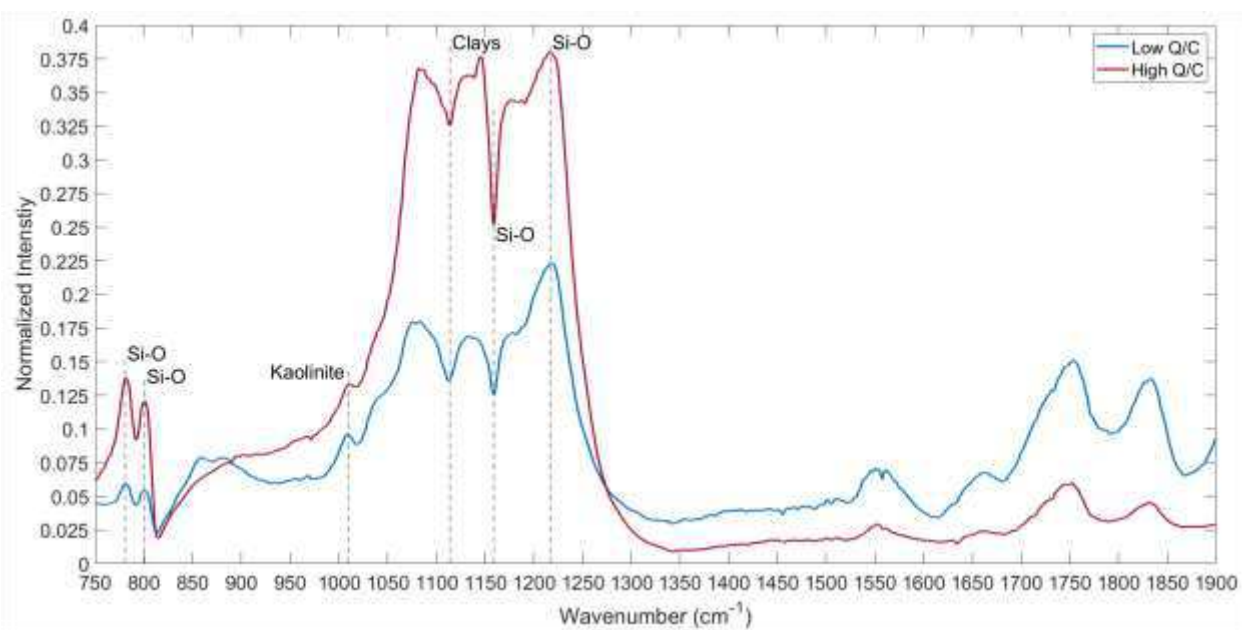
Figure 3. Averaged spectra of low Q/C and high Q/C samples.

The spectral features of the bitumen-free samples are shown in Figure 3. The spectra exhibit two reflection peaks at 780 cm^{-1} and 800 cm^{-1}, respectively. These peaks are attributed to the Si–O band.[14–15] The reflection peak at 1015 cm^{-1} associated to kaolinite, which is a clay, is also shown. The reflection dip at 1120 cm^{-1} is a feature associated to clays.[1] A reflection dip around 1160 cm^{-1} and a strong peak at 1220 cm^{-1}, attributed to the Si–O band of quartz,[15] are also seen in the spectra. The peaks located at 1554 cm^{-1}, 1650 cm^{-1}, 1750 cm^{-1}, and 1834 cm^{-1} are observed in quartz samples with particles of size in the tens of microns range,[16] indicating the particulate nature of the sample.

At first, a qualitative study using principal component analysis (PCA) was performed to identify significant spectral features of quartz and clays in each sample type. This work is focused on the assessment of quartz and clays because they are the most abundant minerals in oil sands ores, but also because the impact of clays on bitumen recovery is significant. PCA is an unsupervised chemometric method used to reduce a set of data of possibly correlated variables into a set of uncorrelated variables called principal components (PC). This method decomposes the dataset matrix into two smaller matrices of scores and loadings which were used to find correlation between the samples. The acquired spectra were preprocessed applying a Savitzky–Golay derivative[17] (first derivative order, 15-point window, and a second-order polynomial).

Then, the data were mean centered. These common pretreatments are used to correct the spectra by changing the scale and the offset, and to highlight the relevant signatures in the spectral dataset. PLS_Toolbox software (Eigenvector) was used to perform the pretreatment and the chemometric modelling. As mentioned in the experimental setup description, the spectra exhibit spectral hopping at 970 cm^{-1}, 1344.7 cm^{-1}, and 1632.4 cm^{-1} caused by the laser diodes switching. The spectral region around these hops usually exhibit low signal-to-noise. Therefore, the 960–980 cm^{-1}, 1330–1350 cm^{-1}, and 1630–1650 cm^{-1} regions were removed before multivariate data analysis.

Principal component analysis was performed on the 55 reflection spectra. Figure 4 shows the PCA score projection of 55 observations and 5000 variables (wavenumber values). The analysis has been performed blindly and the classification of each sample (low and high Q/C) has been disclosed after the chemometric model construction. One can observe a cluster of samples with low quartz to clay ratio which are grouped together as green squares. However, samples with high quartz to clay ratios are scattered on the negative side of the first principal component (PC1) as red diamonds. PC1 has the maximum variance and represents more than 59% of the information. Hence, this component can be used to discriminate the sample spectra
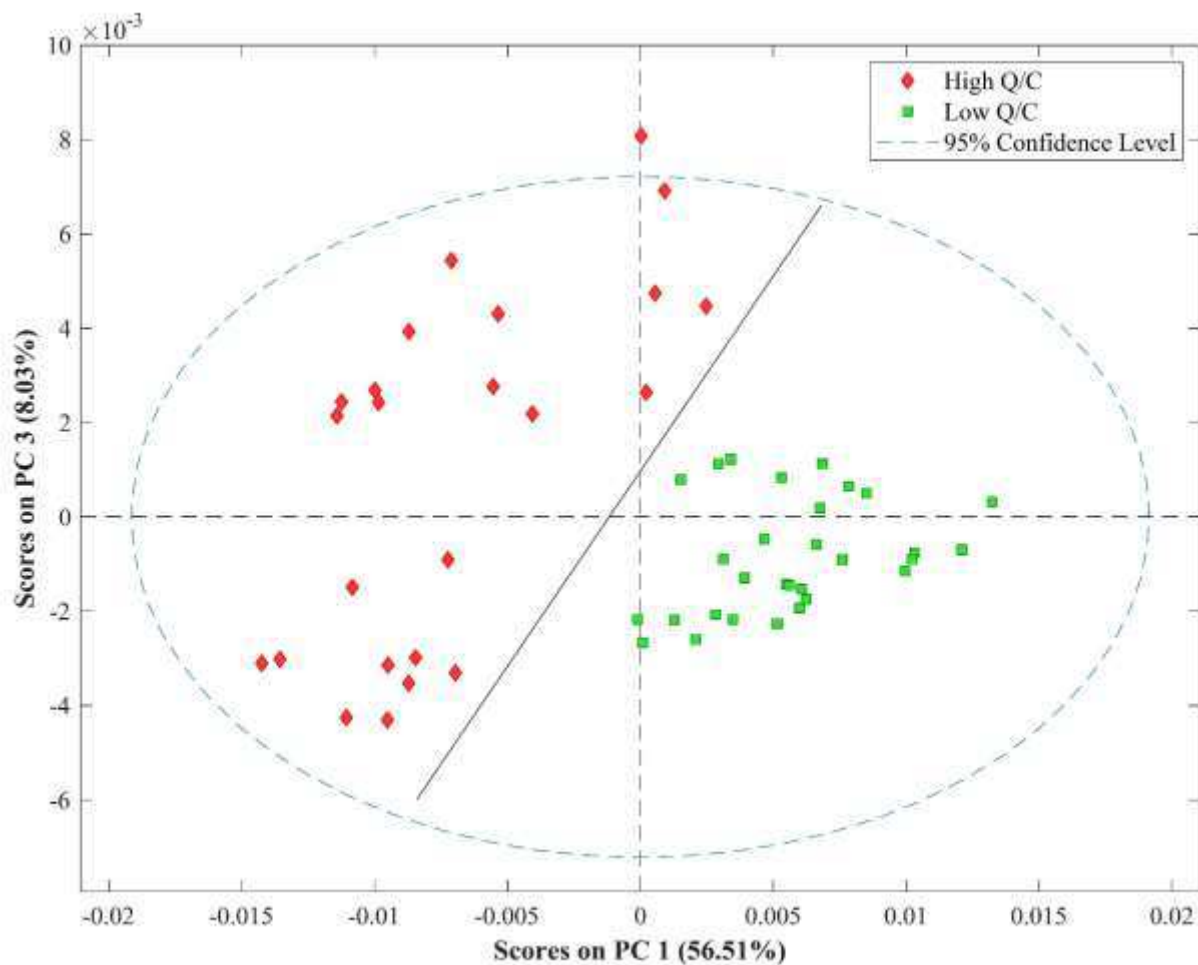
mostly by their quartz to clay ratio.

Figure 4. Score plot of PCA. PC1 versus PC3 for mid-IR spectra based on 750–1900 cm^{-1}.

To understand the meaning of the first principal component, the loadings plot was used. Figure 5 shows the loadings of PC1 as well as the first derivative averaged spectra of samples #1 and #11 which have the lowest and highest quartz to clay ratio respectively. The PC1 loadings show that the feature associated to clays at around 1015 cm^{-1} and 1120 cm^{-1} are anti-correlated with features around 780 cm^{-1}, 800 cm^{-1}, 1160 cm^{-1} and 1220 cm^{-1}, which are associated to quartz. Comparing the PC1 loadings to the averaged spectrum of Sample 1, the features located around 1015 cm^{-1} and 1120 cm^{-1} have the same sign in both spectra. Similarly, the features associated to quartz are inverted compared to the mean. Comparing the PC1 loadings to the mean spectrum of Sample 11 that has the highest quartz to clay ratio, the features located around

$1015\ cm^{-1}$ and $1120\ cm^{-1}$ are weak while the features associated to quartz in both spectra are anti-correlated. This pattern exhibited negative scores for the high Q/C ratio samples in the PCA scores plot of Figure 4. This result agrees with the QXRD results in Table I. Samples with positive PC1 scores contain a low quartz to clay ratio while samples with negative PC1 scores contain a high quartz to clay ratio. Moreover, the observed dispersion of the score data points on the negative side of PC1 can be attributed to spectral variability induced by the large grain size distribution in the high Q/C content samples. Inversely, the scores of the high Q/C samples are less dispersed in the score plot of Figure 4 because these samples are made mostly of homogeneous fines, thanks to the high clay content.
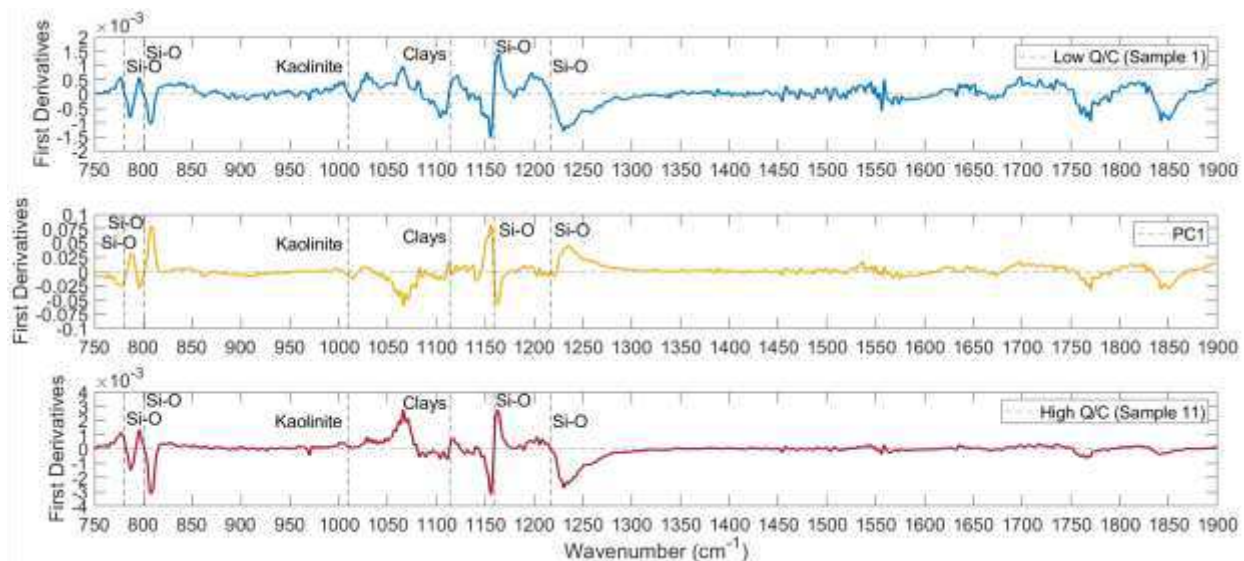

Figure 5. Loadings of PC1, as well as the first derivative averaged spectra of Samples 1 and 11.

Quantification of quartz and total clay content has been performed using a partial least squares (PLS) regression. The PLS regression creates a model linking spectral features to mineralogical content. Five averaged spectra of each sample were used for the quantification in order to assess the precision. The spectra were preprocessed and scaled using Savitzky–Golay derivative and unit variance before building the PLS model. Cross-validation of the model was performed with the venetian blind method[18] and three samples (15 averaged spectra) were used as a test set to evaluate the prediction error. The sample #4 was removed from the calibration set of quartz PLS model. This sample was classified as an outlier because it displayed a value outside the Hotelling's ellipse representing a 95% confidence level for the given PLS model.

PLS regression validation results between QXRD and mid-IR predictions are shown in Figure 6. The model was developed for quartz content and total clay content using four and five latent variables respectively. The root mean square errors of cross-validation (RMSECV) were 3.5% and 3.3% for the quartz content and the total clay content respectively. The root mean square errors of prediction test (RMSEP) were 2.1% and 2.6% for the quartz content and the total clay content respectively. The averaged standard deviations within five measurements were 1.8% and 1.1% for the quartz and the total clay contents respectively. This new approach using a tunable ECQCL source shows a good predictive capability for mineral abundance. However, more samples with a larger variability of quartz and total clay contents are needed. This would improve the quantitative prediction of the technique. The use of such a laser-based approach provides a larger signal to noise ratio thanks to the optical power density of the laser source and offers the capability to do measurements at standoff distances. These conditions are critical for
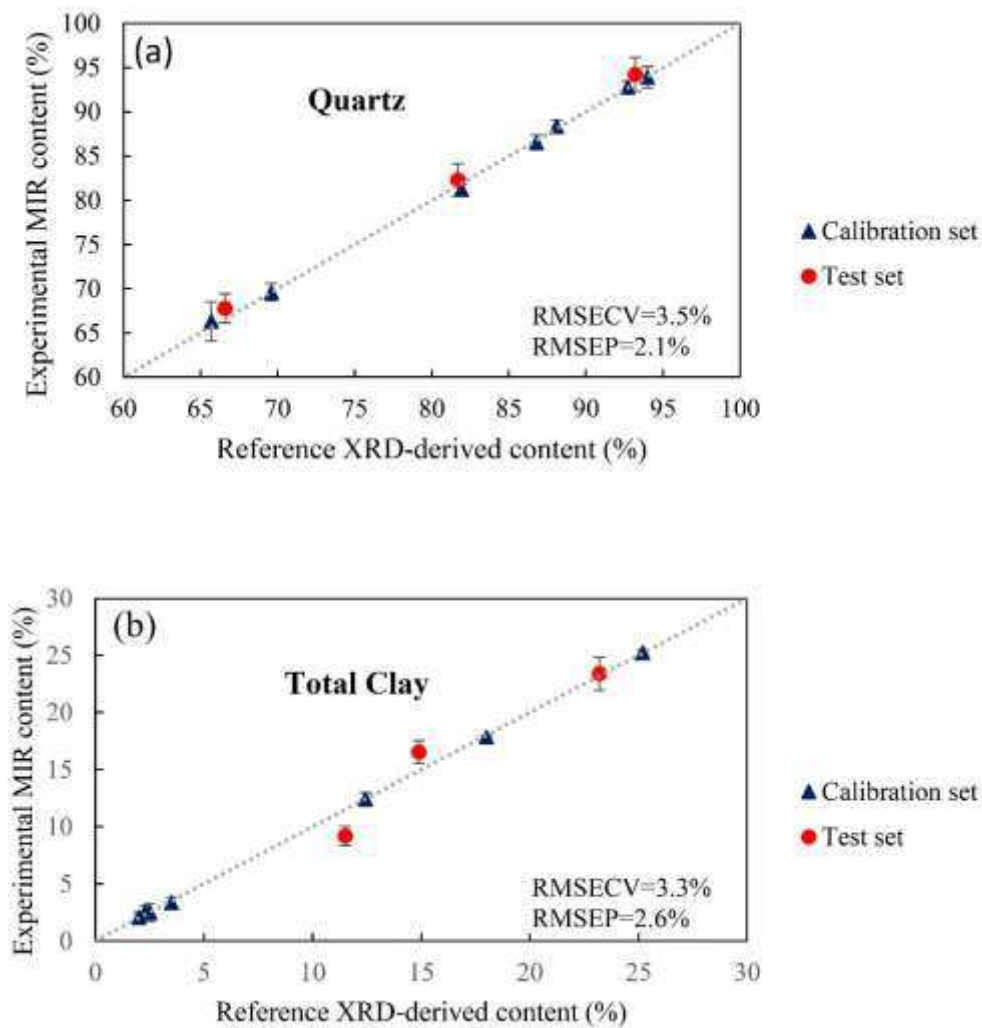
on-line applications.

Figure 6. Comparison of (a) quartz content and (b) total clay content to values predicted from mid-IR data. Dashed line represents 1:1 parity between reference and predicted values. Error bars represent the standard deviation within the five measurements.

Conclusion

The objective of this work was to assess the feasibility of using a tunable ECQCL as a mid–infrared source for mid-IR reflectance spectroscopy of bitumen-free oil sands, and to predict the abundance of quartz and clays in the samples. Results show good correlations with QXRD measurements. The use of a mid-infrared laser-based technique may enable measurements of oil

sands for applications where standoff working distances are necessary such as on-line monitoring. This study is a starting point for developing a real-time technique for the determination of the major mineral contents in oil sands feedstock to monitor and optimize the bitumen recovery process.

Funding

References

1. I. Entezari, B. Rivard, M. Geramian, M.G. Lipsett. "Predicting the Abundance of Clays and Quartz in Oil Sands Using Hyperspectral Measurements". Int. J. Appl. Earth Obs. Geoinform. 2017. 59: 1–8.

2. H.A.W. Kaminsky. Characterization of an Athabasca Oil Sand Ore and Process Streams. [Doctor of Philosophy in Materials Engineering]. University of Alberta, Canada, 2008.

3. A. Harhira, J. El Haddad, A. Blouin, M. Sabsabi. "Rapid Determination of Bitumen Content in Athabasca Oil Sands by Laser-Induced Breakdown Spectroscopy". Energy Fuels. 2018. 32(3): 3189–3193.

4. P. Dougan, K. McDowell. "Sensor Development in Oil Sand Processing". IEEE Industry Applications Society Dynamic Modeling Control Applications for Industry Workshop. Vancouver, BC, Canada; 26–27 May 1997. Pp. 68–73.

5. L. Hvozdara, N. Pennington, M. Kraft, M. Karlowatz, B. Mizaikoff. "Quantum Cascade Lasers for Mid-Infrared Spectroscopy". Vib. Spectrosc. 2002. 30(1): 53–58.

6. Y. Yao, A.J. Hoffman, C.F. Gmachl. "Mid-Infrared Quantum Cascade Lasers". Nat. Photonics. 2012. 6(7): 432.

7. D.T. Childs, R.A. Hogg, D.G. Revin, I.U. Rehman, et al. "Sensitivity Advantage of QCL Tunable-Laser Mid-Infrared Spectroscopy over FT-IR Spectroscopy". Appl. Spectrosc. Rev. 2015. 50(10): 822–839.

8. A. Kosterev, G. Wysocki, Y. Bakhirkin, S. So, et al. "Application of Quantum Cascade Lasers to Trace Gas Analysis". Appl. Phys. B. 2008. 90(2): 165–176.

9. B. Lendl, J. Frank, R. Schindler, A. Müller, et al. "Mid-Infrared Quantum Cascade Lasers for Flow Injection Analysis". Anal. Chem. 2000. 72(7): 1645–1648.

10. M.R. Alcaráz, A. Schwaighofer, C. Kristament, G. Ramer, et al. "External-Cavity Quantum Cascade Laser Spectroscopy for Mid-IR Transmission Measurements of Proteins in Aqueous Solution". Anal. Chem. 2015. 87(13): 6980–6987.

11. N.J. Galán-Freyle, L.C. Pacheco-Londoño, A.D. Román-Ospino, S.P. Hernandez-Rivera. "Applications of Quantum Cascade Laser Spectroscopy in the Analysis of Pharmaceutical Formulations". Appl. Spectrosc. 2016. 70(9): 1511–1519.

12. J. Sun, J. Ding, N. Liu, G. Yang, J. Li. "Detection of Multiple Chemicals Based on External Cavity Quantum Cascade Laser Spectroscopy". Spectrochim. Acta, Part A. 2018. 191: 532–538.

13. F. Vanier, C. Padioleau, M. Sabsabi, A. Blouin. "Combined Laser-Induced Breakdown Spectroscopy and MIR Quantum Cascade Laser Reflectance Spectroscopy for Elemental and Molecular Characterization". Paper presented at: Conference on Lasers and Electro-Optics. San Jose, California; 13 May 2013.

14. J.W. Salisbury, A. Wald. "The Role of Volume Scattering in Reducing Spectral Contrast of Reststrahlen Bands in Spectra of Powdered Minerals". Icarus. 1992. 96(1): 121–128.

15. J. Salisbury, L. Walter, N. Vergo, D. d'Aria. Infrared (2.1–25 mm) Spectra of Minerals. Baltimore, Maryland: Johns Hopkins University Press, 1991. Pp. 267.

16. A. Baldridge, S. Hook, C. Grove, G. Rivera. "The ASTER Spectral Library Version 2.0". Remote Sens. Environ. 2009. 113(4): 711–715.

17. A. Savitzky, M.J. Golay. "Smoothing and Differentiation of Data by Simplified Least Squares Procedures". Anal. Chem. 1964. 36(8): 1627–1639.

18. D. Ballabio, V. Consonni. "Classification Tools in Chemistry. Part 1: Linear Models. PLS-DA". Anal. Methods. 2013. 5(16): 3790–3798.